DOI: 10.1002/ejic.200600816

Small Group IIa–VIa Clusters and Related Systems: A Theoretical Study of Physical Properties, Reactivity, and Electronic Spectra

Martin Srnec*[a] and Rudolf Zahradník[b]

Keywords: Ab initio calculations / Cluster compounds / Structural elucidation

In the monomeric form, the title systems assume unexpected optical properties, and as oligomers they can serve as candidates for molecular devices. In bulk they are attractive in the area of material science. A broad set of quantum chemical methods ranging from density functional theory by the Hartree–Fock method and the Møller–Plesset perturbation theory to the coupled-cluster method, in connection with nonrelativistic Dunning's basis sets as well as with relativistic SDD basis sets were used. Electronic spectra were analyzed by means of time-dependent DFT, with the symmetry-adapted cluster configuration interaction and with the internally contracted multireference configuration interaction. The Douglas–Kroll–Hess quasirelativistic Hamiltonian served as a basis for the estimation of the role of relativistic effects. All the diatomics representing 25 elements of a matrix formed by the combination of group IIa (Be, ..., Ba) with group VIa (O, ..., Po) atoms were characterized by calculated bond length, valence vibration, dipole moment, and the Hartree–Fock frontier orbital energies. Calculated characteristics were confronted with experimental data. The geometry of the oligomers (from dimers through hexamers) was investigated systematically, and the nature of the located stationary points on the respective potential energy surfaces was established. Special attention was paid to the four lightest elements of the group IIa–VIa matrix, i.e. BeO, BeS, MgO, and MgS. As for electronic spectra, the systems of the first column (BeO, ..., BaO), the first row (BeO, ..., BePo), and the systems of the main diagonal (BeO, ..., BaPo) were calculated in the form of monomers and dimers. Analogous calculations were performed for a few group Ia–VIIa, IIIa–Va, IVa–IVa, and IIb–VIa systems. The group IIa–VIa and IIb–VIa diatomics exhibit electronic transitions in the visible region of the spectrum, and the longest wavelength bands are located in the near-infrared region. MgO represents an extreme with the first band appearing at about 3500 cm^{-1}, which strictly speaking makes the use of the Born–Oppenheimer approximation questionable. Whenever experimental transitions are available, the agreement between the calculated and observed band positions is good. Passing from monomers to oligomers is always associated with a significant hypsochromic shift in the first transition.

Introduction

Contemporary electronics, material science, molecular engines, an urgent desire to build computers on the basis of appropriate molecules and macromolecules, and a general tendency to miniaturize prompted us to search for species and materials with the desired properties. These compounds require special physical, chemical, and mechanical characteristics.

For years conjugated organic systems have attracted attention on the basis of the above-mentioned aims and also in connection with the investigation of structure–color relationships. Special interest has been paid to intensively colored species[1a,2] and to systems possessing the longest wavelength transition in the near-infrared region.[1b] Such systems exhibit a very narrow gap between the highest occupied and the lowest unoccupied molecular orbitals (HOMO and LUMO, respectively).

Inorganic systems were, except for various transition-metal complexes, on the periphery of interest. This changed after the discovery of interesting facets (including semiconductivity) of some solids derived, for example, from group IIb–VIa binary compounds, such as, ZnO, ZnS, CdO, and CdS.[3a–3c] Species that are derived from group IIa–VIa elements have received much less attention than the group IIb–VIa compounds. It was shown recently that monomeric forms of group IIa–VIa binary species and small oligomers thereof absorb in the visible and near-infrared regions.[4] Passing from monomers to oligomers of increasing size manifests itself by a hypsochromic shift, which is opposite to that which is known for conjugated organic species.

The group IIa–VIa combination of atoms can be extended to other isoelectronic pairs: groups Ia–VIIa, IIIa–Va, and IVa–IVa. When considering the five elements com-

[a] Department of Molecular Modeling, Institute of Organic Chemistry and Biochemistry, Academy of Sciences of the Czech Republic,
Flemingovo nam.,16610 Prague 6. Czech Republic
E-mail: srnec@uochb.cas.cz
[b] J. Heyrovský of Physical Chemistry, Academy of Sciences of the Czech Republic,
Dolejškova St. 3, 18223 Prague 8. Czech Republic

Supporting information for this article is available on the WWW under http://www.eurjic.org or from the author.

prising the individual groups of the periodic table, 25 species are derived for each of these combinations. The lightest species consists of LiF, BeO, BN, and C_2. These prototypes are followed by 24 molecules; the total number of nonidentical group IVa–IVa combinations amounts to $n(n-1)/2$ (where n is the number of elements in the group), five of them being homonuclear, the remaining, heteronuclear.

In all these instances, 1–10 nm clusters of these parent species represent systems in which the properties are tunable by their size and/or by passing from one element to another element belonging to the same group.

With the group IIa–VIa systems, mostly species containing beryllium and magnesium were investigated. The majority of studies on beryllium compounds, probably because of their toxicity,[5–23] is more theoretical than experimental. Magnesium compounds, mainly MgO, were studied in the context of group IIa–VIa compounds most frequently.[24–50] The number of studies of binary systems containing heavier group IIa metals (Ca, Sr, Ba) is smaller.[24,51–56] Widely investigated were group IIb–VIa systems because of their practical importance. However, only papers having some relevance to systems dealt with in this work are cited.[3a–3c,57–74]

Species of these classes attract attention as nanoparticle[56,62,63,66,68,71,75] materials for quantum dots,[56,58,59] as clusters[24,25,31,43,52,57,59,64a,64b,69] and semiconductors,[3c,57,60,74] and as materials used in the preparation of nanotubes and nanowires.[50,52] The transition between clusters and bulk was investigated.[76] The band structure[7] of BeO and MgO surfaces[26,44a,44b] (and their infrared spectra[37]), as well as doped MgO,[26] were also subjects of scrutiny. Trends in the series BeO through BaO[10] and BeS through BeTe[15,19,23] were described. BeS[6,9,12,17] and MgS[25,33,40] represent materials worth mentioning. Not only closed-shell parent systems, but also radical–ions[13,14,27a,29,35,36] derived from them were subjects of studies, sometimes by means of photoelectron spectroscopy.[27a,38] The electron affinity of BeO is so high that complexes with rare gases were described.[8]

In addition to the currently widely used Hartree–Fock, Møller–Plesset, and coupled-cluster methods (vide infra), density functional theory[10,11,22,34,49,53,73] and empirical potentials[24,46,51] served to describe large systems, clusters in particular. A full configuration interaction (CI) was used to study[5] the electronic structure of BeO.

Electronic spectra investigations[16,27b,27c,34,48,56] involved mainly MgO (size-dependency of the MgO clusters[42]). In ref.[54] spectra of CaO, SrO, and BaO were analyzed. A correlation was found to exist between the energy of the Khon–Sham orbitals and the excitation energies.[77] Infrared spectra of MgO[37] and BeO complexes with noble gases[21,22] are available.

Calculations of dissociation energies (e.g. for MgO,[28] MgO^+, and SrO^+ in ref.[28]), as well as heats of formation (BeO, MgO, CaO),[20] still represent a rather demanding task.

In this paper, we utilize various quantum chemical methods to determine the structural and electronic characteristics of monomeric through hexameric group IIa–VIa species (group IIa: Be through Ba; group VIa: O through Po) and to determine how these characteristics vary with different elements, cluster size, and geometrical structure. We focus on the following features: (1) Screening structural and physical properties of all 25 group IIa–VIa monomers. (2) Detailing the study of the properties of the four lightest MX monomers (M = Be, Mg; X = O, S). (3) Testing relativistic effects on the properties of a representative molecule, CaSe. (4) Characterizing geometries of oligomeric isomers. (5) Characterizing electronic spectra for the most stable isomers. (6) Evaluating trends of physical characteristics in a series of oligomers.

Computational Details

Quantum chemical methods were used for the computation of the structural and physical properties of selected group IIa–VIa diatomics MX, their oligomers M_iX_i (from dimers to hexamers, i = 2,.., 6), and for some related systems by using the Gaussian 03 program package.[78]

In the first part concerning diatomics, attention was focused on screening the bond lengths, the harmonic valence vibrations, the electric dipole moments, and frontier orbital energies. The following computational schemes were used: density functional theory (DFT) with the B3LYP exchange-correlation functional, the Hartree–Fock method (HF), and the second-order Møller–Plesset perturbation theory (MP2). Calculations were performed for all the matrix elements (diatomics) of the group IIa–VIa matrix. Relativistic pseudopotentials were used throughout the calculations so as to describe relativistic effects, which increase with Z^4 and Z^2 (Z – proton number) for inner and outer electrons, respectively. The SDD basis sets[79a] are appropriate for this purpose and are available in the Gaussian 03 standard library. Analysis of the wavefunctions was carried out by means of the CASSCF method[79b] by using the MOLPRO 02 program.[79c]

The second part relates to the four lightest members of the group IIa–VIa matrix. These diatomics were extensively characterized by means of the DFT method using nonrelativistic Dunning's basis sets[80a–80c] (cc-pVXZ from double-zeta to quintuple-zeta) and the calculated characteristics were almost always extrapolated to the complete basis set (CBS) limit according to the (quasi)linear dependency between the physical characteristics and the reciprocals of the total number of basis set functions.[81] Unless otherwise stated, the geometry optimization of the oligomers was always performed at the B3LYP/cc-pVTZ level. The positions of the first electronic valence (the longest wavelength) bands of these species were estimated by means of the time-dependent density functional method (TD–B3LYP). These results were then compared with the experimental data (if available) and with the results of two more robust methods, namely, the symmetry-adapted cluster configuration interaction (SAC–CI),[82] including single and double excitations, and the internally contracted multireference config-

uration interaction (icMRCI),[83a,83b] also with single and double excitations. Specification of the reference configuration space related to icMRCI calculations will be mentioned with concrete instances. The electronic transitions were fitted with equal-weighted Gauss/Lorentz curves with half-maximum widths of 1000 cm^{-1}; the Frank–Condon factors were not considered.

In the third part, we were interested in the trends of some structural and spectral features along the horizontal (the first row), the vertical (the first column), and the main diagonal directions of the group IIa–VIa matrix (Figure 1). The second-order Douglas–Kroll–Hess (DKH)[84a–84c] scalar quasirelativistic Hamiltonian was explored in the local spin density basis set DZVP[85] and the large-core SDD pseudopotential technique (vide supra), both within the B3LYP procedure. The DKH method neglects the two-electron relativistic corrections and also spin-orbit coupling. This method is based on the free-particle Foldy–Wouthuysen (FW)[84d] transformation, which separates the electronic and positronic solutions of the Dirac equation by the unitary transformation of the Dirac–Coulomb–Breit Hamiltonian. The approximate scheme of the DKH method applies the free-particle FW transformation to the molecular bare-nucleus Hamiltonian and, moreover, also applies additional transformations to remove off-diagonal Hamiltonian elements, which results in variational stability.

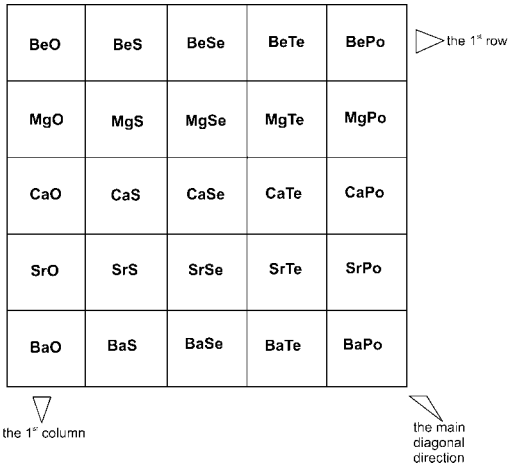

Figure 1. Diatomics formed by a combination of atoms of groups IIa and VIa. Three main directions are indicated.

The adiabatic and vertical ionization potentials (I_a and I_v, respectively) and the adiabatic and vertical electron affinities (A_a and A_v, respectively) are defined as follows [Equations (1), (2), (3), and (4)]:

$$I_a = E_{M_iX_i^{+-}}\left(M_iX_i^{+-}\right) - E_{M_iX_i}\left(M_iX_i\right) + \frac{1}{2}h\sum_j^{3N-6}\left[\nu_j\left(M_iX_i^{++}\right) - \nu_j\left(M_iX_i\right)\right] \quad (1)$$

$$I_v = E_{M_iX_i^{+-}}\left(M_iX_i\right) - E_{M_iX_i}\left(M_iX_i\right) \quad (2)$$

$$A_a = E_{M_iX_i^{--}}\left(M_iX_i^{--}\right) - E_{M_iX_i}\left(M_iX_i\right) + \frac{1}{2}h\sum_j^{3N-6}\left[\nu_j\left(M_iX_i^{--}\right) - \nu_j\left(M_iX_i\right)\right] \quad (3)$$

$$A_v = E_{M_iX_i^{--}}\left(M_iX_i\right) - E_{M_iX_i}\left(M_iX_i\right) \quad (4)$$

where the lower index and the index in parentheses specify chemical species and the structure, which was optimized, respectively. The adiabatic forms include the zero-point energy (ZPE) corrections; ν_j stands for the jth vibrational mode. The energy of the open-shell species was calculated by unrestricted methods.

The energy of formation of the oligomers was calculated by means of the following expression [Equation (5)]:

$$\Delta E = (iE_M + iE_x - E_{M_iX_i})/i \quad (5)$$

Equation (5) permits the estimation of the relative stability of the isomers. The basis set superposition error (BSSE) was calculated by using the function counterpoise method[86] and included throughout. It necessarily tends to zero when approaching complete basis sets.

The Mulliken population analysis was used for semiquantitative estimates of partial charges at the atoms.

Results and Discussion

Monomers: Screening of Structural and Selected Physical Properties

The ground state of all the studied species is a singlet state. The only uncertainty is related to BaPo. Again, a singlet represents the ground state with the SDD basis set (S–T split amounts to 3.6 kcal mol^{-1} with B3LYP). With the ECP-CRENBL[87] basis set, however, the opposite is true (T–S split is equal to 13.5 kcal mol^{-1} with B3LYP). The semiquantitative estimates of the S–T splittings for all group IIa–VIa species are available on request from the authors.

Bond lengths, valence vibrations, dipole moments, and frontier orbital energies for 25 group IIa–VIa diatomics are summarized in Figure 2. The bond length dependencies (A, B) are monotonic and reflect the empirical statement that passing from the first-row element to its nearest neighbor manifests itself roughly with the same degree of change relative to that found by passing between the second and the fifth period. The B3LYP, HF, and MP2 bond length courses overlap significantly. Average deviations between calculated and observed[88] bond lengths for the species of the first matrix column amount to 29 (B3LYP/SDD), 24 (HF/SDD), and 70 pm (MP2/SDD).

Dependences C and D in Figure 2 have to do with harmonic wavenumbers ($\tilde{\nu}$), which decrease monotonically in the columns and rows of the matrix. By contrast, force constants of magnesium chalcogenides exert minima. This agrees well with the remarkable reactivity of MgO.[31] Again, the features of the species that include first-row ele-

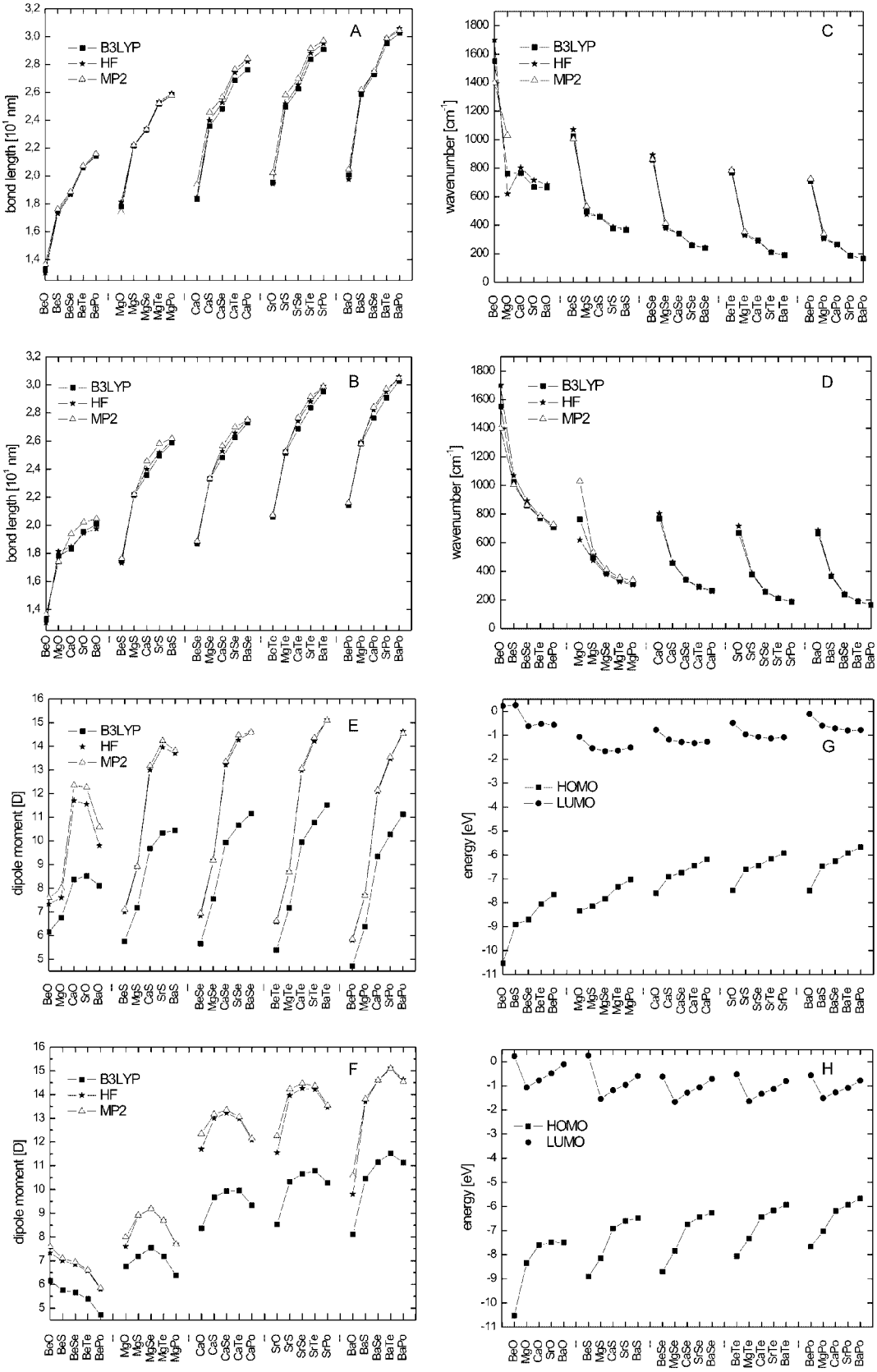

Figure 2. Trends of bond lengths, ℓ(A, B), wavenumbers of valence vibrations, $\tilde{\nu}$(C, D), electric dipole moments, μ(E, F), and energies of frontier orbitals, E(G, H) for 25 group IIa–VIa diatomics: oxides, sulfides, selenides, tellurides, polonides of beryllium, magnesium, calcium, strontium, and barium, respectively. Computational methods and units used are indicated in the graphs. The DFT (B3LYP), HF, and MP2 methods were used with pseudopotential SDD basis sets. HF frontier orbital energies correspond, except for signs, to Koopmans' ionization potential and electron affinity.

ments are shifted from the data for the rest of the systems. This is particularly obvious for BeO. There is a fair agreement between B3LYP/SDD and experimental wavenumbers for species of the first matrix column. The largest deviation was observed for MgO (16%), whereas for BaO it amounted to only 0.6%.

The dipole moments (Figure 2, E and F) indicate significantly the ionic nature of all the systems. There is a rather dramatic difference between the B3LYP and the HF and MP2 values (always with the SDD basis sets). Reasonable agreement between B3LYP and highly accurate theoretical values for BeO (6.16 and 6.15–6.25 D,[18] respectively) and BeS (5.76 and 5.19 D,[17] respectively) suggest the superiority of the B3LYP estimates with respect to the two other procedures. This confirms our previous experience.[81] In contrast to dependencies for species in columns, the dependencies in the rows exerts (except for beryllium chalcogenides) well-developed maxima for selenides or tellurides. On the whole, the B3LYP dipole moments assume values between 5 and 11 D.

The HF frontier orbital energies (Figure 2, G and H) represent, within the framework of the Koopmans' theorem, the first vertical ionization potential (HOMO) and the first vertical electron affinity (LUMO). The ionization potentials decrease and the electron affinities increase in the rows of the matrix. Dependencies for electron affinities

Table 1. Calculated bond lengths (R_e), dipole moments (μ), wavenumber of valence vibrations ($\tilde{\nu}$), vertical ionization potential (I_v), vertical electron affinity (A_v), and formation enthalpy corresponding to the process $MX(^1\Sigma^+) = M(^1S) + X(^1D)$ for BeO, BeS, MgO, and MgS. The B3LYP and MP2 methods were obtained for Dunnig's basis sets (n; cc-pVXZ with X = D, T, Q, 5). Only in a few cases were very sophisticated calculated values used as a benchmark instead of experimental values.

		B3LYP					
Species	*n*	R_e [10^{-10} m]	μ [D]	$\tilde{\nu}$ [cm^{-1}]	I_v [eV]	A_v [eV]	ΔE[a] [kJ/mol]
BeO	D	1.3381	5.71	1510	9.85	2.00	–686
	T	1.3233	6.11	1551	9.90	2.13	–721
	Q	1.3193	6.27	1554	10.13	2.14	–729
	5	1.3195	6.39	1551	10.15	2.17	–731
	liter.	1.331[c]	6.15–6.25[b]	1487[c]	10.1 ± 0.4[c]	–	–544 ± 50[d]
BeS	D	1.7540	4.90	1000	9.08	2.13	–478
	T	1.7414	5.24	1009	9.24	2.24	–490
	Q	1.7375	5.32	1012	9.25	2.28	–493
	5	1.7374	5.34	1012	9.25	2.31	–493
	liter.	1.742[c]	5.19[e]	998[c]	–	–	–
MgO	D	1.7493	6.28	814	7.61	1.72	–448
	T	1.7430	6.86	822	7.76	1.77	–471
	Q	1.7388	7.19	826	7.81	1.83	–483
	5	1.7343	7.35	826	7.83	1.84	–489
	liter.	1.749[c]	–	785[c]	8.76 ± 0.22[c]	–	–594 ± 42[c]
MgS	D	2.1620	6.88	523	7.68	1.94	–342
	T	2.1514	7.30	527	7.80	2.00	–353
	Q	2.1490	7.46	527	7.81	2.05	–356
	5	2.1414	7.52	530	7.82	2.05	–358
	liter.	2.143[c]	–	529[c]	–	–	–
		MP2					
BeO	D	1.3746	7.17	1337	9.88	1.65	–696
	T	1.3535	7.36	1406	10.11	1.87	–760
	Q	1.3480	7.48	1414	10.29	1.94	–780
	5	1.3479	7.56	1414	10.40	1.99	–788
	liter.	1.331[c]	6.15–6.25[b]	1487[c]	10.1 ± 0.4[c]	–	–544 ± 50[d]
BeS	D	1.7710	6.24	991	9.09		–470
	T	1.7592	6.42	994	9.20		–504
	Q	1.7522	6.48	1002	9.30		–519
	5	1.7500	6.49	1004	9.34		–526
	liter.	1.742[c]	5.19[e]	998[c]	–		–
MgO	D	1.7341	7.74	1068	8.73		–502
	T	1.7377	8.43	1033	8.98		–564
	Q	1.7398	8.81	1022	9.08		–587
	5	1.7413	9.04	1012	9.14		–598
	liter.	1.749[c]	–	785[c]	8.76 ± 0.22[c]		–594 ± 42[c]
MgS	D	2.1662	8.75	559	7.39	1.63	–351
	T	2.1556	9.08	561	7.69	1.82	–388
	Q	2.1514	9.25	562	7.78	1.89	–403
	5	2.1474	9.32	564	7.82	1.91	–410
	liter.	2.143[c]	–	529[c]	–	–	–

[a] Formation enthalpy $MX(^1\Sigma^+) = M(^1S) + X(^1D)$. [b] Value recommended on the basis of theoretical results.[18] [c] Taken from Huber–Herzberg collection.[88] [d] Taken from experimental work.[96] [e] Theoretical value from ref.[17]

along the columns exert clear minima for the Mg-containing species.

The differences between the calculated (HF, Koopmans' theorem) and observed[89] ionization potentials for the species in the first column ($\Delta I = I_{calcd.} - I_{exp.}$) amount to 0.42, –0.43, –0.80, –0.88, and –0.89 eV. Notably, CI vectors in the CASSCF approach suggest an admixture of 7 to 10% of excited configurations in the ground states.

The BeO, BeS, MgO, and MgS Systems

The results of DFT and MP2 calculations for bond length, dipole moment, valence vibration, vertical ionization potential and electron affinity, and heat of formation for the title diatomics are presented in Table 1. The bond lengths and valence vibrations can be obtained for the set of diatomics under study with satisfactory precision.

The MP2 CBS bond lengths, when compared to experimental values, exhibit an average deviation of 0.7 pm. The B3LYP CBS values underestimate the experiment by 1.1 pm. The average deviation of wavenumbers is smallest for the B3LYP procedure and amounts in the CBS limit to 36 cm^{-1}.

Vertical ionization potentials and electron affinities were obtained from Equations (2) and (4). The overall agreement is satisfactory, which also applies to HF data (not included in Table 1) with the use of Koopmans' theorem.

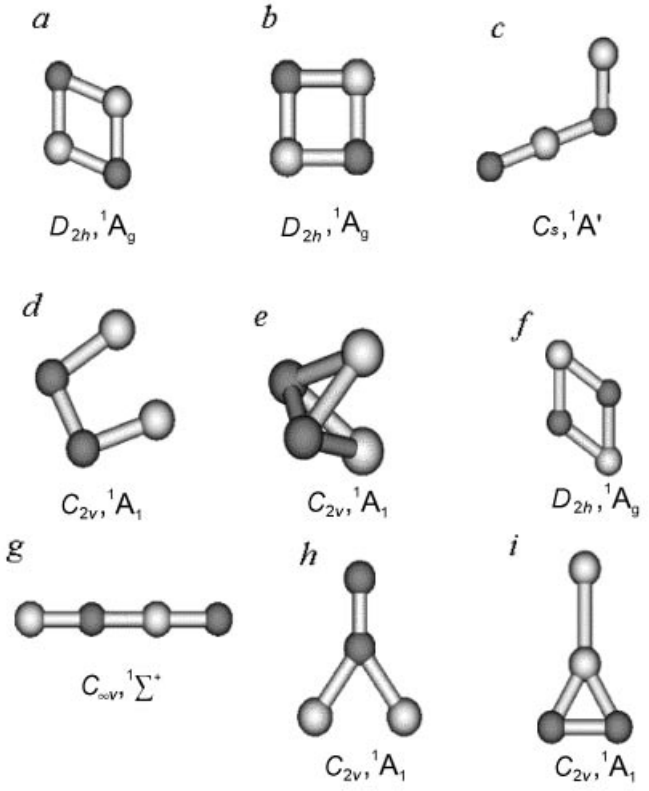

		a	b	c	d	e	f	g	h	i
Be_2O_2	A	GM	LM	LM	LM	LM	LM	-	S1	S1
	B	No	No	No	94;5	74;25	58;40	-	-	-
	C	0.0	157	268	546	552	270	-	-	-
Be_2S_2	A	GM	LM	LM	LM	S1	S1	S1	LM	S1
	B	No	No	No	95;2	-	-	-	97;1	-
	C	0.0	277	312	350	-	-	-	564	-
Mg_2O_2	A	GM	LM	-	LM	-	LM	S1	LM	LM
	B	97;1	97;1	-	58;41	-	58:42	-	87;6	96;2
	C	0.0	36	-	214	-	214	-	397	410
Mg_2S_2	A	GM	LM	LM	LM	LM	S1	S1	LM	LM
	B	No	No	No	89;5	82;16	-	-	88;6	96:4
	C	0.0	125	23	224	222	-	-	339	303

Figure 3. Localized stationary points on the B3LYP/cc-pVDZ energy hypersurfaces of Be_2O_2, Be_2S_2, Mg_2O_2, and Mg_2S_2. Each of them is described by symmetry point group and electronic ground state. White and grey balls correspond to metal (Be, Mg) and chalcogen (O, S) atoms, respectively. In the presented table, basic information about the isomers found is collected in the following way: A – nature of stationary point (GM – global minimum, LM – local minimum, S*n* – saddle point of *n*th order); B – multireference wavefunction character of isomer [percentage ratio of the two most dominant wavefunctions; analysis with CASSCF(4,6)]; C – relative energies of dimer isomers (in $kJ\,mol^{-1}$).

Calcium Selenide: Testing System for Relativistic Contribution Estimate

This system consisting of the fourth row elements was used for estimating the role of relativistic effects. The comparison was made with nonrelativistic B3LYP/cc-pVTZ and quasirelativistic DKH-B3LYP/cc-pVTZ methods. The latter method includes those components of relativistic corrections which can be considered essential. The calculations were performed for the monomer ($^1A_{1g}$) and the dimer ($^1B_{3u}$) and concerned molecular geometry, heat of formation, the first adiabatic ionization potential and electron affinity, wavenumbers of vibrational modes, and excitation energies for the longest wavelength electronic transition. The results are transparent: except for the heats of formation, the changes are not significant. In the case of the (negative) heats of formation, the relativistic values are about 20% bigger than the nonrelativistic ones.

Structure of Oligomers M_iX_i (M = Be, Mg; X = O, S; *i* = 2–6)

Dimers: Stationary points on the respective potential energy surfaces have been obtained by the energy minimization of numerous initial structures selected on the basis of chemical intuition and fantasy. The nature of the located stationary points was ascertained by means of the eigenvalue signs of the respective Hessians. This made it possible to distinguish global and local minima and the first- and higher-order saddle points. Except for minima, only the first-order saddle points are of chemical relevance, and they represent activated complexes of the Eyring absolute rate theory. The structures investigated with the dimers and detailed information on the nature of the located stationary points is presented in Figure 3. For the sake of simplicity, we concluded that the rhombic structure with acute angles at chalcogens represented a global minimum not only with Be_2O_2, Be_2S_2, Mg_2O_2, and Mg_2S_2 but in general also with analogue dimers. We observe that the opposite is true with group IIIa–Va dimers: acute angles are associated with the metal atoms.[90] Moreover, all these species represent single-reference systems. Figure 3 shows that a local minimum is only a little higher in energy than the global minimum. However, in the case of Mg_2O_2, structure *b* is about 36 kJ mol^{-1} above the global minimum, and with Mg_2S_2, structre *c* is 23 kJ mol^{-1} above the global minimum.

Passing from monomers to dimers is accompanied by a lengthening of the M–X bond by 16, 18, 12, and 17 pm for Be_2O_2, Be_2S_2, Mg_2O_2, and Mg_2S_2, respectively (B3LYP/cc-pVDZ). The softer nature of these bonds is indicated by the b_{1u} harmonic normal vibrational modes of the dimers.

Trimers: Despite great effort, it seems that the only significant minimum on the PES of these systems are hexagons possessing the D_{3h} structure. They are products of strong electrostatic (head–tail) interactions of three building units. It is tempting to try to ascribe the stability of the D_{3h} structures to a kind of aromaticity. Although there is a significant formal similarity between the systems under study and moieties such as benzene and cyclic C_6 (D_{3h}), the great difference in the electronegativity of the atoms that form building units (e.g. Be and O) reduces delocalization considerably. Again, the angles at the chalcogen atoms of the trimers are smaller than those at metal atoms. The structure of the group IIIa–Va and group IIb–VIa species is analogous.[69,90] Chemical intuition has strong support in molecular dynamics. We have been able to show by a simulated annealing procedure[91] the superiority of the D_{3h} structure for the four dimers which were thoroughly studied. Heavier trimers from the group IIIa–Va matrix prefer[90] a three-dimensional structure, which was ascribed to the low-lying d orbitals and energy diminution due to higher coordination numbers. We might add that linear trimers represent saddle points of the higher order. The bond lengths in trimers are equal 146.7, 190.9, 184.0, and 229.9 pm for the BeO, BeS, MgO, and MgS bonds, respectively. This means that all the bonds are about 3 pm shorter than the analogous bonds in the dimers.

Tetramers: We have been able to localize three stationary points with all four building units under study (Figure 4). The BeO tetramer is the most stable in a planar octagonal form (D_{4h}). Mg_4O_4 and Mg_4S_4 assume a heterocubic structure (T_d); with Be_4S_4 the situation is somewhat more involved. A minimum of D_{2d} symmetry passes through an extremely low-lying transition state of D_{4h} symmetry into an equivalent D_{2d} system. The B3LYP/cc-pVTZ barrier

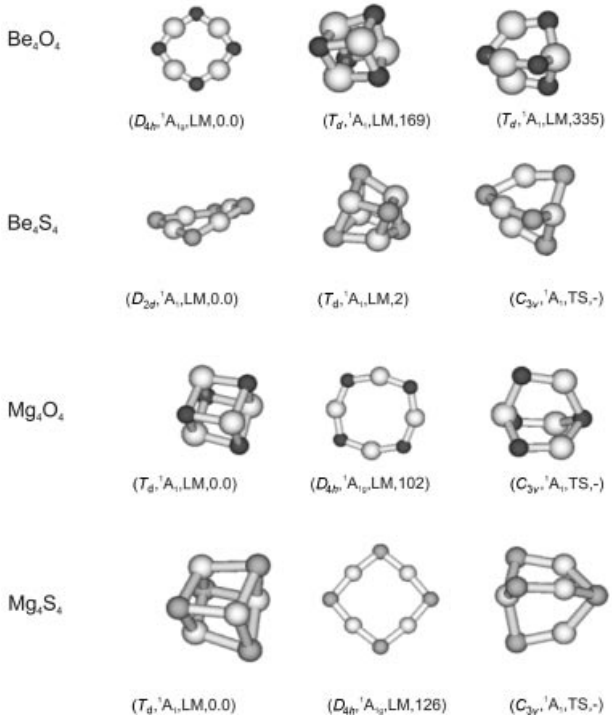

Figure 4. Localized stationary points on the B3LYP/cc-pVDZ energy hypersurfaces of Be_4O_4, Be_4S_4, Mg_4O_4, and Mg_4S_4. Symmetry group, electronic state, nature of the stationary point, and relative energy (kJ mol^{-1}) with respect to the most stable isomer are in parentheses. Dark spheres stand for chalcogen. Local minima (LM) and transition states (TS).

amounts to 0.5 kJ mol^{-1} and can be neglected at room temperature. The A_1 ground state is not degenerate and therefore the deviation from coplanarity cannot be attributed to the Jahn–Teller effect. However, pseudo Jahn–Teller distortion is applicable, which is supported by arguments in ref.[60] The HOMO (b_{1u}) and LUMO (a_{1g}) orbitals in the D_{2d} geometry are transformed into a_1 orbitals, which are capable of mixing. The mixing is probably not very pronounced because of the large energy gap between these orbitals estimated on the basis of the first electronic transition (3.9 eV; TD-B3LYP/cc-pVDZ). At this level, the energy difference between the D_{2d} and T_d structures is so small that the order of isomers can be changed when passing to a higher level of theory.

The Be_4O_4, Mg_4O_4, and Mg_4S_4 clusters with D_{4h} symmetry and Be_4S_4 with D_{2d} symmetry have bond lengths equal to 145.3, 182.6, 228.6 and 190.1 pm, respectively (B3LYP/cc-pVDZ), which correspond roughly to the values of the bond lengths in the trimers. The contraction of bond lengths with respect to those of dimers could indicate heteroaromatic behavior of the rings. The bond lengths in the most stable isomers of Mg_4O_4 and Mg_4S_4 (both with T_d symmetry) are 195.7 and 243.0 pm, which is in agreement with the expected increase in bond lengths when passing to bulk: $(MgO)_\infty$, 210.6 and $(MgS)_\infty$, 260.0 pm.

Pentamers: Localized stationary points are summarized in Figure 5. Only Be_5O_5 assumes a planar monocyclic structure (decagon) with D_{5h} symmetry. Another isomer has a naphthalene-like structure with C_{2v} symmetry. The other three pentamers are most stable in a nonplanar structure (C_s). Monocyclic structures with Be_5S_5 are nonplanar (C_s), whereas with Mg_5O_5 they are planar (D_{5h}). The D_{5h} structure of Mg_5S_5 is a second-order saddle point. The addition of one electron to the monocyclic nonplanar C_s structure of Be_5S_5 causes planarization of the ring (D_{5h}) accompanied by reduction of the Be–Be distance. Ladder structures have been localized with pentamers except Be_5O_5, but they have little chemical relevance.

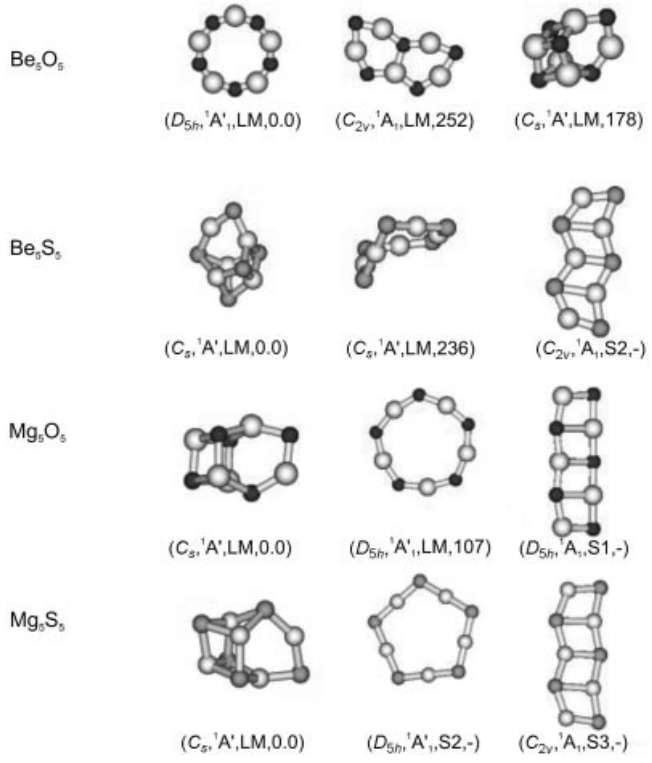

Figure 5. Localized stationary points on the B3LYP/cc-pVDZ energy hypersurfaces of Be_5O_5, Be_5S_5, Mg_5O_5, and Mg_5S_5. Symmetry group, electronic state, nature of the stationary point, and relative energy (kJ mol^{-1}) with respect to the most stable isomer are in parentheses. Dark spheres stand for chalcogen. Local minima (LM) and saddle points of the *n*th order (S*n*).

Hexamers: Ten local minima are among 16-localized stationary points for the four systems under study (Figure 6). With all hexamers, the most stable forms have D_{3d} structure, which consists of six-membered cycles in a stacking arrangement. This form represents a building unit of wurzite crystals, which concerns beryllium oxide and sulfide. Magnesium compounds crystallize frequently into a cubic structure, which, at the level of hexamers, is represented by the D_{2h} structure. It can be considered a kind of "sandwich" consisting of three stable rhombic units. Only Mg_6O_6 and Mg_6S_6 represent local minima; the beryllium containing systems of the D_{2h} structure are saddle points.

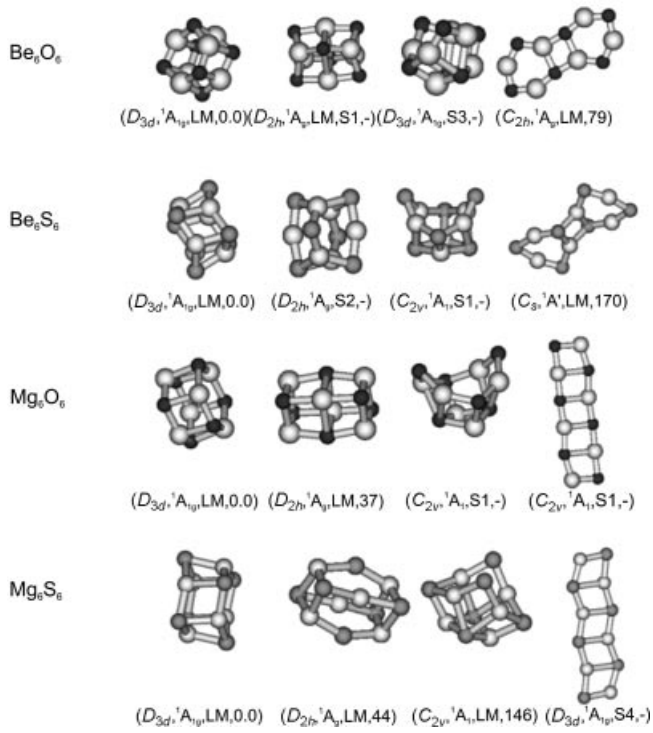

Figure 6. Localized stationary points on the B3LYP/cc-pVDZ energy hypersurfaces of Be_6O_6, Be_6S_6, Mg_6O_6, and Mg_6S_6. Symmetry group, electronic state, nature of the stationary point, and relative energy (kJ mol^{-1}) with respect to the most stable isomer are in parentheses. Dark spheres stand for chalcogen. Local minima (LM) and saddle points of the *n*th order (S*n*).

Bowl-like C_{2v} structures consisting of tetragons, in contrast to Zn_6S_6 and Zn_6Se_6 clusters,[60] are not stable species; they are just saddle points. Mg_6S_6 assumes a special posi-

tion by being a local minimum. This might be tentatively ascribed to the d orbitals of S and Mg, which stabilize systems with atoms having high coordination numbers.

The Be_6O_6 system exists with a local minimum (C_{2h}) consisting of two hexagons and one (connecting) rhombic motif. Therefore, there is a formal resemblance between this system and diphenylene in the benzenoid hydrocarbon series. With reference to Be_6S_6, this C_{2h} structure converges to a nonplanar system with C_s structure, whereas Mg_6O_6 and Mg_6S_6 pass into a ladder structure of a saddle-point nature.

Time consumption connected with the B3LYP/cc-pVDZ geometry optimization of hexamers can be reduced considerably by using the PM3 preoptimization.[92]

Electronic Spectra

We believe we have shown convincingly[4] that for BeO, BeS, MgO, and MgS the longest wavelength transitions calculated by TD-B3LYP/cc-pVDZ and SAC-CI(SD)/cc-pVDZ mutually agree satisfactorily. The same is true when

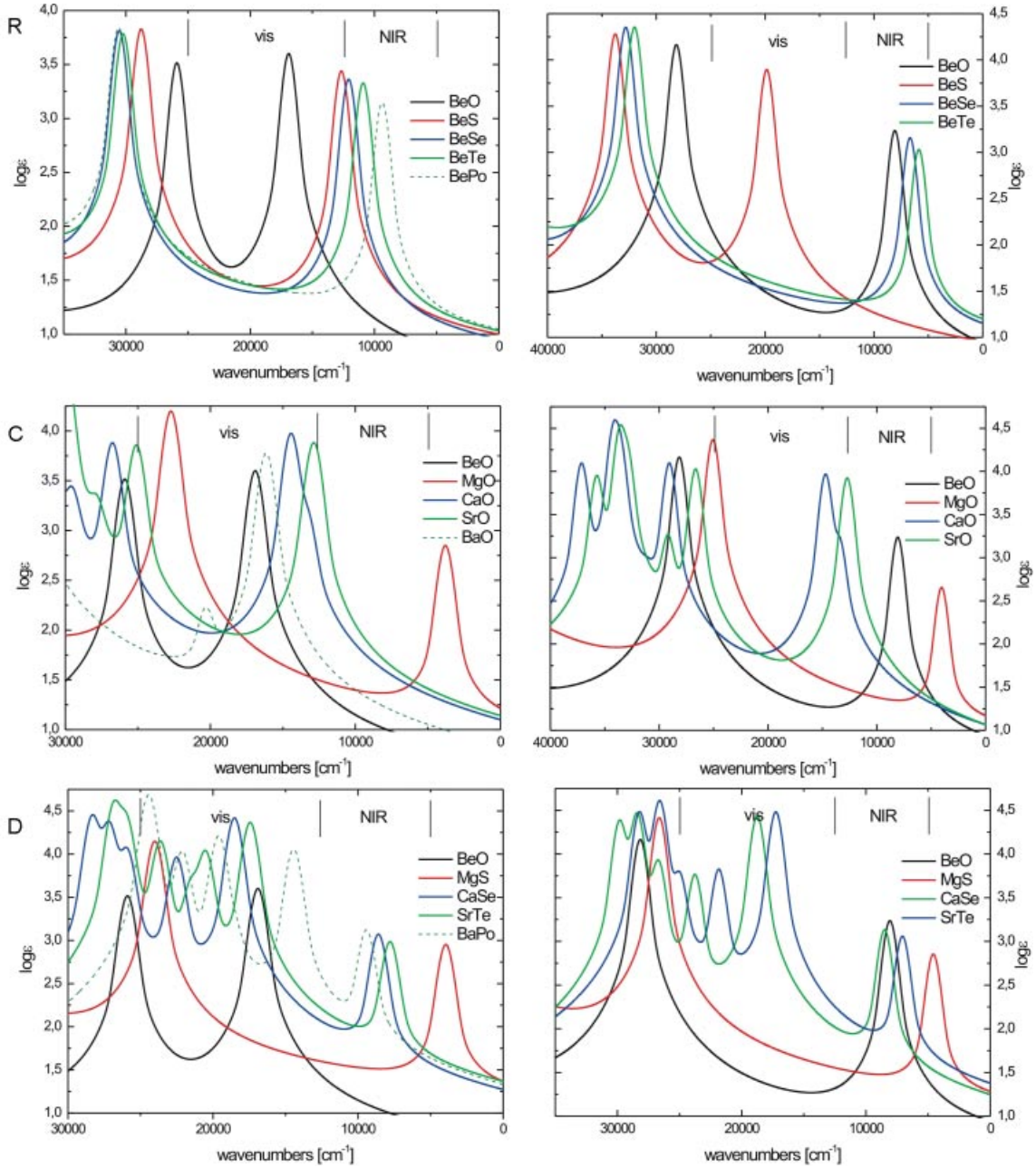

Figure 7. Computed electronic spectra of the group IIa–VIa diatomics at the TD-B3LYP/SDD (the left column) and DKH-B3LYP/VDZP (the right column) level. Three directions in the group IIa–VIa matrix are considered (the first column, C; the first row, R; the main diagonal, D). The regions of visible (vis) and near-infrared regions (NIR) are indicated.

comparing calculated and observed[4] band positions in the near-infrared and visible regions of the spectrum. An analogous statement is valid for dimers of the above-mentioned diatomics, except that there are no experimental data available. In all instances, passing from monomer to dimer is accompanied by a very large hypsochromic shift. Moreover, it has been shown with the monomers that the use of the icMRCI procedure produces similar results. Although passing from DZ to TZ brings about an improvement in all three methods relative to the experimental values, the TD-B3LYP/cc-pVDZ method is well-suited and a relatively economic procedure for good semiquantitative predictions.

The order of transitions with oxides forming the first column (BeO, ..., BaO) remains unchanged ($X^1\Sigma^+ \rightarrow A^1\Pi$, $X^1\Sigma^+ \rightarrow B^1\Sigma^+$, $X^1\Sigma^+ \rightarrow B^1\Pi$, and $X^1\Sigma^+ \rightarrow C^1\Sigma^+$) between BeO and CaO. For SrO, the two first transitions are approximately equal in energy, and with BaO, the first band connected with the $\Sigma^+ \rightarrow \Sigma^+$ transition is observed.

Instead of calculating the electronic spectroscopic data for all matrix elements and the dimers thereof, we dealt with systems of the first column (BeO, ..., BaO), of the first row (BeO, ..., BePo), and with systems formed from the main diagonal (BeO, ..., BaPo) (cf. Figure 1). The respective theoretical absorption curves are depicted in Figure 7 for di-

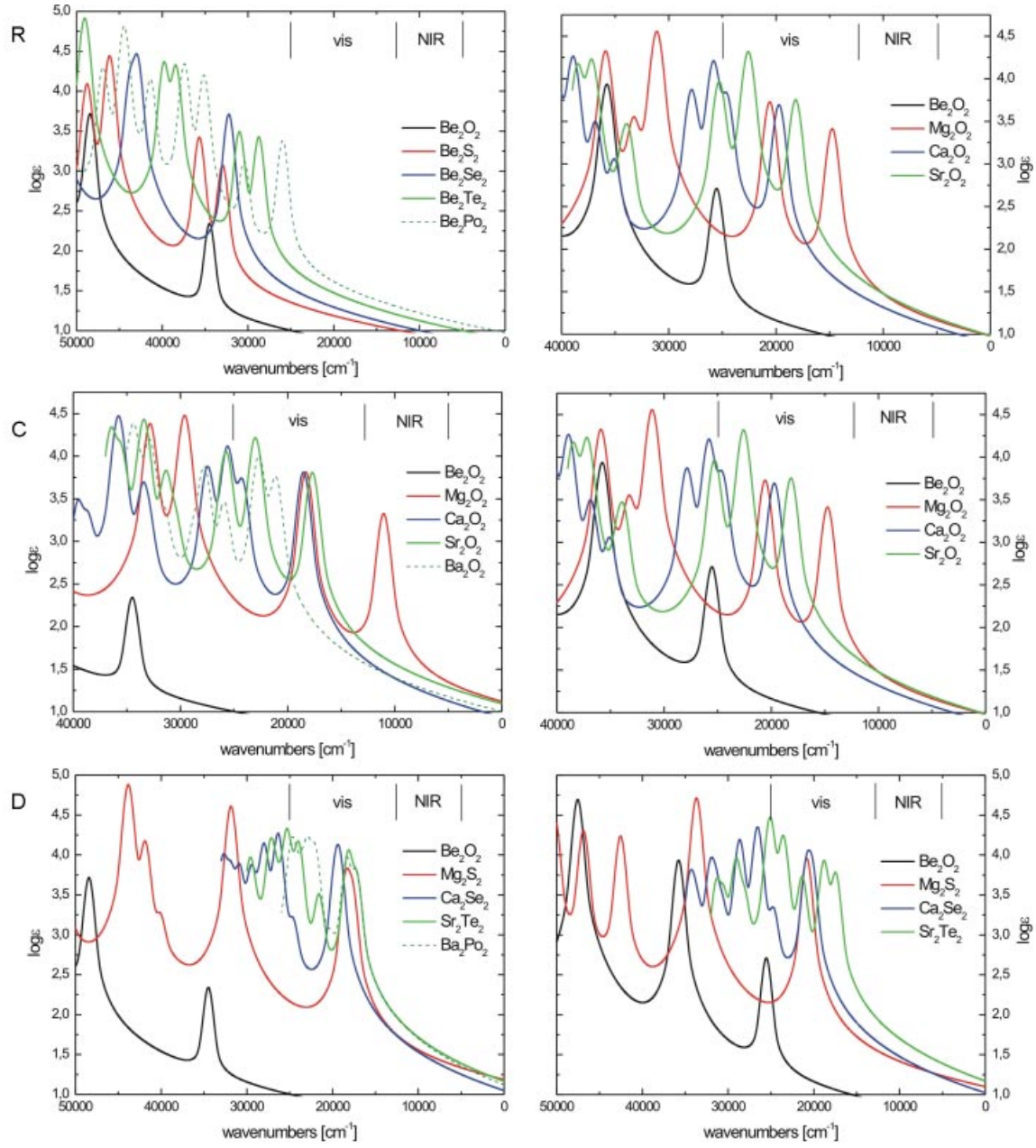

Figure 8. Computed electronic spectra of dimers of the group IIa–VIa diatomics at the TD-B3LYP/SDD (the left column) and DKH-B3LYP/VDZP (the right column) level. Three directions in the group IIa–VIa matrix are considered (the first column, C; the first row, R; the main diagonal, D). The regions of visible (vis) and near-infrared regions (NIR) are indicated.

atomics and in Figure 8 for their dimers. On the basis of comparison between calculated and observed band positions for all group IIa oxides and BeS and MgS, it is possible to say that the curves in Figures 7 and 8 offer a realistic picture of the electronic spectra. The first absorption band is either in the near-infrared region (in the majority of cases) or in the visible region. The overall picture is quite similar for both theoretical levels used, but the DKH procedure seems to be more reliable. However, the only real failure of the pseudopotential basis set (SDD) is for BeO and its dimer.

Calculated electronic spectra for the most stable pairs of isomers of the dimers, tetramers, and hexamers of MgO suggest the possibility to use this type of spectroscopy for structure elucidation (Supporting Information, see Figure S1).

Trends in Physical Characteristics in Series of Oligomers

A summarizing note on the geometry of clusters will be augmented by remarks on ionization potentials and elec-

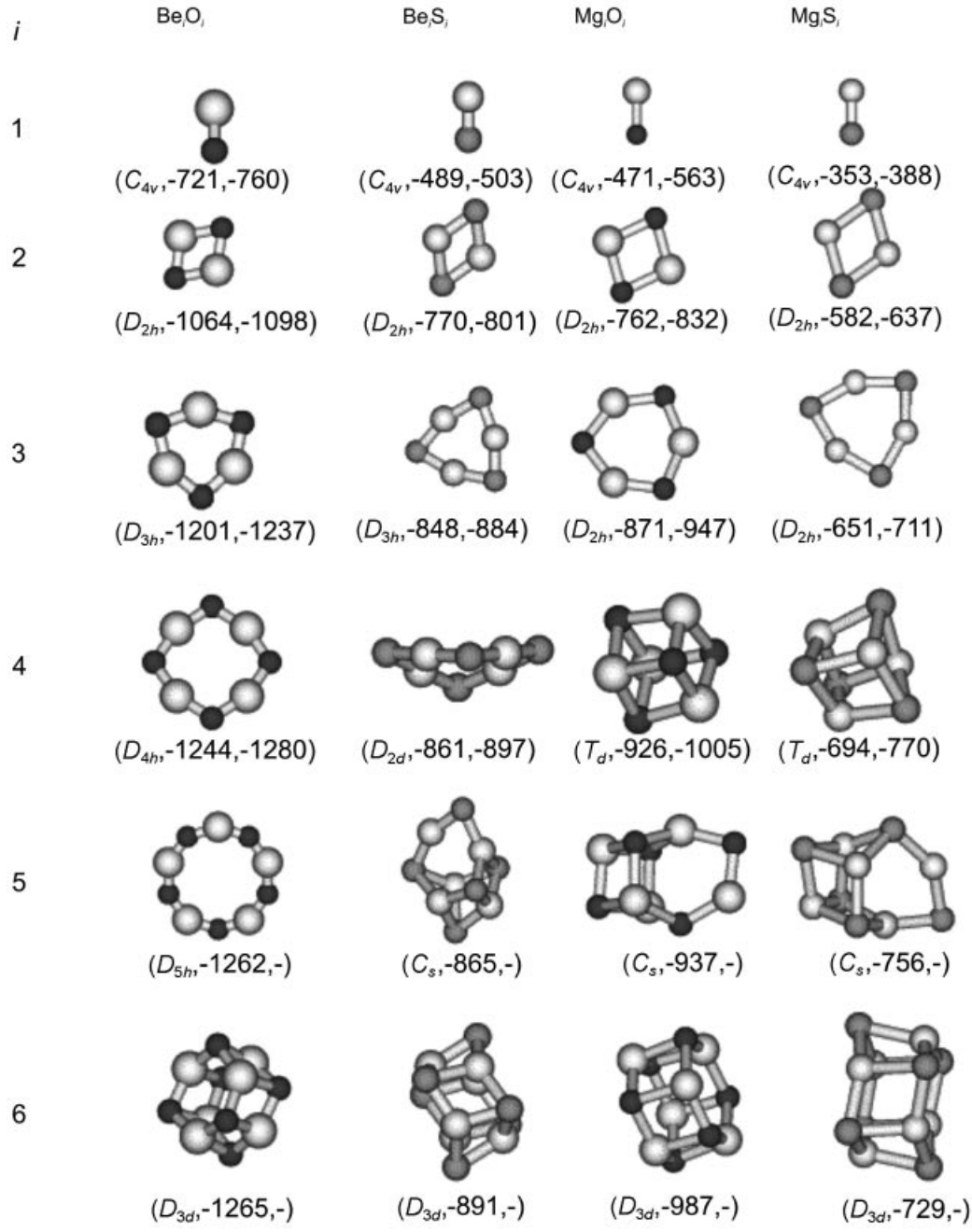

Figure 9. Structure of global minima of $(MX)_i$ on the respective energy hypersurface. Symmetry group and calculated energy of formation, ΔE (B3LYP/cc-pVTZ and MP2/cc-pVTZ) per MX unit (kJ mol^{-1}). Basis set superposition error is included. Dark spheres mean chalcogen.

tron affinities. Assumed global minima are summed up in Figure 9. Notably, higher oligomers consist of rhombic and hexagonal motifs. Specific energies of formation of oligomers, that is energies per monomer unit, are defined by Equation (5). The two sets of formation energies (DFT and MP2) are available up to tetramer and differ by about 5%. It is hardly possible to say which of the methods should be preferred. Obviously, however, it is desirable to have for small oligomers such a comparison available and, for more extensive systems, the DFT procedure represents the only, remarkably reliable, chance. Increasing specific formation energy suggests the increasing stability of larger oligomers and also their decreasing reactivity. It is known from the literature[3c,69] that attempts to obtain cohesion energy of a crystal by extrapolating the formation energy of small clusters are not successful. Internal energy of BeO and MgO crystals are 1180 and 995 kJ mol^{-1}.[93]

Ionization potentials, I, and electron affinities, A, are valuable characteristics in several respects. The BeO clusters are used as representatives. Adiabatic and vertical values are defined by Equations (1)–(4). In opposition to the formation energies, the plots of I and A against the cluster size are not smooth (Figure 10). Relative maxima with ionization potentials correspond to i = 3 and 5, whereas minima are at i = 2, 4, and 6. This suggests that there is stabilization of cycles with 6 and 10 atoms; minima on the plot are connected with 4, 8, and 12 atoms in the ring. It is at least formally an analogy to the aromatic and nonaromatic cyclic, conjugated hydrocarbons. The same was observed in the BN series, that is aromaticity with $(BN)_3$ and $(BN)_5$.[94] the adiabatic and vertical values differ very little, which indicates an absence of dramatic geometry changes after removal or addition of an electron. The trends are the same for both methods used.

In Table S1 (Supporting Information), we summarize the values of the partial charges at the metal atoms for the oligomers depicted in Figure 9. We wish to underline two points: (1) The ionic character increases with cluster size, which correlates to a hypsochromic shift in the electronic spectra (vide infra). The partial charges are also significantly influenced by the coordination environment and that is apparent in the series of Be_iO_i, i = 1–6. Only the Be_6O_6 system has a different coordination number of atoms and is not consistent with the smooth trend for i = 1–5. (2) The MgO molecule exerts significant covalency; the growth of ionic character for the MgO clusters with increasing i is most dramatic among species included in Figure 9.

The dependence of the positions on the longest wavelength bands for oxides and sulfides of beryllium and magnesium is shown in Figure 11. The only structurally homogeneous series for i = 1–5 is BeO: the first band of the cyclic structures exhibits a dramatic hypsochromic shift from about 10 000 (i = 1) to 60 000 cm^{-1} (i = 5). The bathochromic shift when passing from pentamer to hexamer is, no doubt, due to structural changes, namely to the transition to a three-dimensional structure (D_{3d}). The courses for the remaining three systems support the plausibility of this assumption because a change from hypsochromicity to bathochromicity manifests itself by passing from trimer to tetramer, which coincides with passing from planarity to three-dimensional structures.

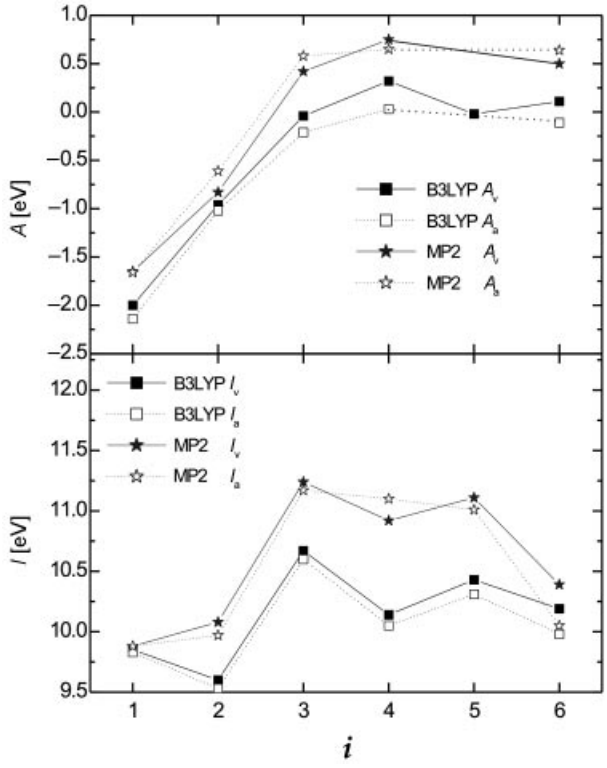

Figure 10. Vertical and adiabatic ionization potentials and electron affinities plotted against the size of the most stable $(BeO)_i$ oligomers (eV). In adiabatic values zero-point energy is included [cf. Equations (1)–(4)]. B3LYP/cc-pVDZ (squares: full-vertical, empty-adiabatic), MP2/cc-pVDZ (stars: full-vertical, empty-adiabatic) calculations.

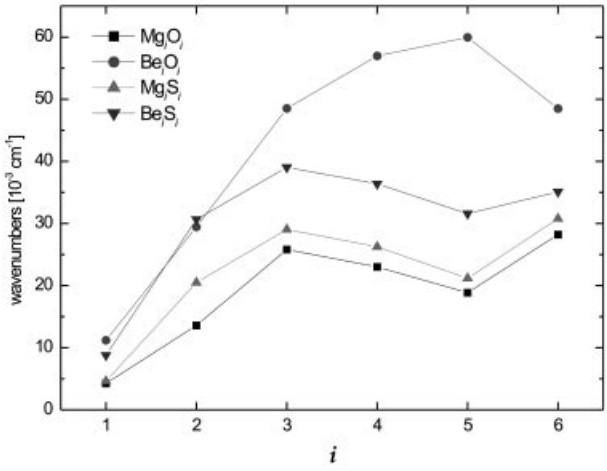

Figure 11. The shift in the position of the longest wavelength absorption band in the electronic spectra in four series of systems ranging from monomer up to hexamer. The calculations have been performed at the TD-B3LYP/cc-pVTZ level.

A remarkably close correlation exists between TD DFT excitation energies (for transitions which dominate the HOMO–LUMO excitation) and differences of Khon–Sham

eigenvalues, which result from the solution of Kohn–Sham equations with the B3LYP functional. Recently, such correlations were observed and analyzed.[70,77] This finding is valuable because it makes estimates of the first-band position on the basis of a calculation possible, which, for extensive systems, are significantly more economic than complete TD DFT calculations.

Finally, let us briefly comment on the first and second excitation energies in the isoelectronic series of diatomics related to the second row of the periodic table. The wavenumbers [cm^{-1}] are as follows: LiF: 40530, 45600; BeO: 9410, 21250; BN: 27880, –; and C_2: 720, –. These values were obtained at the TD-B3LYP/cc-pVTZ level (LiF, BeO) or taken from ref.[95] (BN, C_2). Except for group IIa–VIa species, in all instances the passing from monomers (diatomics) to dimers is associated with a bathochromic shift.

The related group IIb–VIa diatomics MX (M = Zn, Cd, Hg; X = O, S) exert the first two bands in similar regions as the group IIa–VIa species. Whereas the first peak (TD-B3LYP/cc-pVTZ [cm^{-1}]) is located in the near-infrared or infrared region (ZnO: 5570; ZnS: 5040; CdO: 2810; CdS: 2810; HgO: 3350; HgS: 1960) with very low intensity, the second one, which is more intensive by about two orders of magnitude, is shifted to the near-UV region (ZnO: 31470; ZnS: 32290; CdO: 28400; CdS: 28730; HgO: 32560; HgS: 32635).

Conclusions

Although the group IIa–VIa system in bulk does not attract the attention of many chemists, which is (partly) due to a big gap between valence and conduction bands and their chemical inertness, the opposite is true for group IIa–VIa diatomics and clusters thereof. We found that the diatomics unexpectedly exert the first absorption band in the near-infrared or visible regions and this band is progressively shifted toward shorter wavelengths with growing cluster size.

The structural variety of group IIa–VIa species is significantly limited by strong ionic interaction of metal–chalcogen poles. Therefore, the most stable structures of larger clusters could be considered as a combination of a few, rhombic and hexagonal, patterns.

We feel strongly that catalytic properties of bulk surfaces could be enhanced by deposing cluster-like structures. In this work, we tried to demonstrate how electronic characteristics are tunable by varying the metal and chalcogen, cluster size, and isomerization. We hope that the group IIa–VIa species can be valuable for new molecular devices similar to the group IIb–VIa species.

Supporting Information (see footnote on the first page of this article): Electronic spectra and partial charges at metal atoms.

Acknowledgments

Our sincere thanks are due to Mr. J. Novotney and Mrs. R. Žohová for significant help with the preparation of the final version of the manuscript.

[1] a) J. Fabian, R. Zahradník, *Angew. Chem. Int. Ed. Engl.* **1989**, *28*, 677; b) D. F. Perepichka, M. R. Bryce, *Angew. Chem. Int. Ed.* **2005**, *44*, 5370.
[2] a) J. Koutecký, R. Zahradník, *Collect. Czech. Chem. Commun.* **1960**, *25*, 811.
[3] a) Ch. W. Bauschlicher Jr, S. R. Langhoff, *Chem. Phys. Lett.* **1986**, *126*, 163; b) T. Hiratani, K. Konishi, *Angew. Chem. Int. Ed.* **2004**, *43*, 5943; c) J. M. Matxain, J. M. Mercero, J. E. Fowler, J. M. Ugalde, *J. Phys. Chem. A* **2003**, *107*, 9918.
[4] M. Srnec, R. Zahradník, *Chem. Phys. Lett.* **2005**, *407*, 283.
[5] Ch. W. Bauschlicher Jr, S. R. Langhoff, *Theor. Chim. Acta* **1988**, *73*, 43.
[6] N. Benosman, N. Amrane, S. Méçabih, H. Aourag, *Physica B* **2001**, *304*, 214.
[7] K. J. Chang, S. Froyen, M. L. Cohen, *J. Phys. C: Solid State Phys.* **1983**, *16*, 3475.
[8] G. Frenking, W. Koch, J. Gauss, D. Cremer, *J. Am. Chem. Soc.* **1988**, *110*, 8007.
[9] O. Fuchs, L. Weinhardt, C. Heske, E. Umbach, A. Fleszar, C. Bostedt, L. J. Terminello, R. C. C. Perera, *Advanced Light Source Comp.* **2001**.
[10] P. Fuentealba, A. Savin, *J. Phys. Chem. A* **2000**, *104*, 10882.
[11] Y. H. Hu, *J. Am. Chem. Soc.* **2003**, *125*, 4388.
[12] D.-Y. Hwang, A. M. Mebel, *J. Am. Chem. Soc.* **2000**, *122*, 11406.
[13] K. D. Jordan, *Chem. Phys. Lett.* **1978**, *54*, 320.
[14] K. D. Jordan, *Chem. Phys. Lett.* **1979**, *62*, 143.
[15] G. Landwehr, A. Waag, F. Fischer, H.-J. Lugauer, K. Schüll, *Physica E* **1998**, *3*, 158.
[16] S. R. Langhoff, Ch. W. Bauschlicher Jr, H. Partridge, *J. Chem. Phys.* **1986**, *84*, 4474.
[17] J. Noga, T. Pluta, *Chem. Phys. Lett.* **1997**, *264*, 101.
[18] V. Parasuk, P. Neogrády, H. Lischka, M. Urban, *J. Phys. Chem.* **1996**, *100*, 6325.
[19] R. L. Sarkar, S. Chatterjee, *J. Phys. C: Solid State Phys.* **1977**, *10*, 57.
[20] M. B. Sullivan, M. A. Iron, P. C. Redfern, J. M. L. Martin, L. A. Curtiss, L. Radom, *J. Phys. Chem. A* **2003**, *107*, 5617.
[21] C. A. Thompson, L. Andrews, *J. Am. Chem. Soc.* **1994**, *116*, 423.
[22] A. A. Thompson, L. Andrews, *J. Phys. Chem.* **1996**, *100*, 12214.
[23] A. Waag, Th. Litz, F. Fischer, H.-J. Lugauer, T. Baron, K. Shüll, U. Zehnder, T. Gerhard, U. Lunz, M. Keim, G. Reuscher, G. Landwehr, *J. Crystal Growth* **1998**, *184/185*, 1.
[24] A. Aguado, J. M. López, *J. Phys. Chem. B* **2000**, *104*, 8398.
[25] M. A. Al-Laham, G. W. Trucks, K. Raghavachari, *J. Chem. Phys.* **1992**, *96*, 1137.
[26] A. L. Almeida, J. B. L. Martins, E. Longo, N. C. Furtado, C. A. Taft, J. R. Sambrano, W. A. Lester Jr, *Int. J. Quantum Chem.* **2001**, *84*, 705.
[27] a) Ch. W. Bauschlicher Jr, H. Partridge, *Chem. Phys. Lett.* **2001**, *342*, 441; b) Ch. W. Bauschlicher Jr, B. H. Lengsfield III, D. M. Silver, D. R. Yarkony, *J. Chem. Phys.* **1981**, *74*, 2379; c) Ch. W. Bauschlicher Jr, D. M. Silver, D. R. Yarkony, *J. Chem. Phys.* **1980**, *73*, 2867.
[28] Ch. W. Bauschlicher Jr, B. H. Lengsfield III, B. Liu, *J. Chem. Phys.* **1982**, *77*, 4084.
[29] D. K. Böhme, H. Schwarz, *Angew. Chem. Int. Ed.* **2005**, *44*, 2.
[30] A. I. Boldyrev, J. Simons, P. R. von Schleyer, *Chem. Phys. Lett.* **1995**, *233*, 266.
[31] A. I. Boldyrev, J. Simons, *J. Phys. Chem.* **1996**, *100*, 8023.
[32] A. I. Boldyrev, I. L. Shamovsky, P. R. von Schleyer, *J. Am. Chem. Soc.* **1992**, *114*, 6469.
[33] C. Bradford, C. B. O'Donnell, B. Urbaszek, A. Balocchi, C. Morhain, K. A. Prior, B. C. Cavenett, *Appl. Phys. Lett.* **2000**, *76*, 3929.
[34] G. Cappellini, F. Finocchi, S. Bouette-Russo, C. Noguera, *Comput. Mater. Sci.* **2001**, *20*, 401.

[35] N. F. Dalleska, P. B. Armentrout, *Int. J. Mass Spectrosc. Ion Processes.* **1994**, *134*, 203.
[36] M. Gutowski, P. Skurski, X. Li, L.-S. Wang, *Phys. Rev. Lett.* **2000**, *85*, 3145.
[37] E. Kagi, T. Hirano, S. Takano, K. Kawaguchi, *J. Mol. Spectrosc.* **1994**, *168*, 109.
[38] J. H. Kim, L.-S. Wang, H. L. de Clerq, C. A. Fancher, O. C. Thomas, K. H. Bowen, *J. Chem. Phys. A* **2001**, *105*, 5709.
[39] S. Kohiki, M. Arai, H. Yoshikawa, S. Fukushima, *J. Phys. Chem. B* **1999**, *103*, 5296.
[40] A. Lichanot, A. Dargelos, C. Larrieu, *Solid State Commun.* **1994**, *90*, 189.
[41] E. Lucas, S. Decker, A. Khaleel, A. Seitz, S. Fultz, A. Ponce, W. Li, C. Carnes, K. J. Klabunde, *Chem. Eur. J.* **2001**, *7*, 2505.
[42] I. Onal, S. Senkan, *Industrial & Engineering Chem. Res.* **1997**, *36*, 4028.
[43] J. M. Recio, R. Pandey, A. Ayuela, A. B. Kunz, *J. Chem. Phys.* **1993**, *98*, 4783.
[44] a) D. Ricci, C. Di Valentin, G. Pacchioni, P. V. Sushko, A. L. Shluger, E. Giamello, *J. Am. Chem. Soc.* **2003**, *125*, 738; b) D. Ricci, G. Pacchioni, P. V. Sushko, A. Shluger, *J. Chem. Phys.* **2002**, *117*, 2844.
[45] C. Roberts, R. L. Johnston, *Phys. Chem. Chem. Phys.* **2001**, *3*, 5024.
[46] A. J. Rowley, P. Jemmer, M. Wilson, P. A. Madden, *J. Chem. Phys.* **1998**, *108*, 10209.
[47] M. Stener, G. Fronzoni, R. De Francesco, *Chem. Phys.* **2004**, *298*, 141.
[48] S. Stankic, M. Müller, O. Diwald, M. Sterrer, E. Knözinger, J. Bernardi, *Angew. Chem. Int. Ed.* **2005**, *44*, 4917.
[49] S. Veliah, R. Pandey, Y. S. Li, J. M. Newsam, B. Vessal, *Chem. Phys. Lett.* **1995**, *53*, 235.
[50] Y. Wu, H. Yan, M. Huang, B. Messer, J. H. Song, P. Yang, *Chem. Eur. J.* **2002**, *8*, 1261.
[51] A. Aguado, L. Bernasconi, P. A. Madden, *J. Chem. Phys.* **2003**, *118*, 5704.
[52] A. R. Armstrong, J. Canales, P. G. Bruce, *Angew. Chem. Int. Ed.* **2004**, *43*, 4899.
[53] P. Cortona, *Int. J. Quantum Chem.* **2004**, *99*, 828.
[54] R. W. Field, *J. Chem. Phys.* **1974**, *60*, 2400.
[55] C. N. Jarman, R. A. Hailey, P. F. Bernath, *J. Chem. Phys.* **1992**, *96*, 5571.
[56] C. Wang, K. Tang, Q. Yang, C. An, B. Hai, G. Shen, Y. Qian, *Chem. Phys. Lett.* **2002**, *351*, 385.
[57] A. P. Alivisatos, *J. Phys. Chem.* **1996**, *100*, 13226.
[58] R. E. Bailey, S. Nie, *J. Am. Chem. Soc.* **2003**, *125*, 7100.
[59] D. Battaglia, J. J. Li, Y. Wang, X. Peng, *Angew. Chem. Int. Ed.* **2003**, *42*, 5035.
[60] P. Deglmann, R. Ahlrichs, K. Tsereteli, *J. Chem. Phys.* **2002**, *116*, 1585.
[61] K. Gokhberg, A. Glozman, E. Lifshitz, T. Maniv, M. C. Schlamp, P. Alivisatos, *J. Chem. Phys.* **2002**, *117*, 2909.
[62] J. Hu, Y. Bando, J. Zhan, D. Golberg, *Angew. Chem. Int. Ed.* **2004**, *43*, 4606.
[63] J. Hu, Y. Bando, D. Golberg, *Small* **2005**, *1*, 95.
[64] a) J.-O. Joswig, G. Seifert, T. A. Niehaus, M. Springborg, *J. Phys. Chem. B* **2003**, *107*, 2897; b) J.-O. Joswig, M. Springborg, G. Seifert, *J. Phys. Chem. B* **2000**, *104*, 2617.
[65] M. Kurtz, J. Strunk, O. Hinrichsen, M. Muhler, K. Fink, B. Meyer, C. Wöll, *Angew. Chem. Int. Ed.* **2005**, *44*, 2790.
[66] Q. Li, C. Wang, *J. Am. Chem. Soc.* **2003**, *125*, 9892.
[67] J. J. Li, Y. A. Wang, W. Guo, J. C. Keay, T. D. Mishima, M. B. Johnson, X. Peng, *J. Am. Chem. Soc.* **2003**, *125*, 12567.
[68] Z. Li, Y. Ding, Y. Xiong, Q. Yang, Y. Xie, *Chem. Eur. J.* **2004**, *10*, 5823.
[69] J. Matxain, J. M. Mercero, J. E. Fowler, J. M. Ugalde, *J. Phys. Chem. A* **2004**, *108*, 10502.
[70] J. M. Matxain, J. M. Mercero, J. E. Fowler, J. M. Ugalde, *J. Am. Chem. Soc.* **2003**, *125*, 9494.
[71] T. Nann, J. Riegler, *Chem. Eur. J.* **2002**, *8*, 4791.
[72] C. Pacholski, A. Kornowski, H. Weller, *Angew. Chem. Int. Ed.* **2002**, *41*, 1188.
[73] E. Spanó, S. Hamad, C. R. A. Catlow, *J. Phys. Chem. B* **2003**, *107*, 10337.
[74] H. Weller, *Angew. Chem. Int. Ed. Engl.* **1993**, *32*, 41.
[75] U. Drechsler, B. Erdogan, V. M. Rotello, *Chem. Eur. J.* **2004**, *10*, 5570.
[76] A. Pramann, K. Rademann, *Chem. Phys. Lett.* **2001**, *347*, 46.
[77] A. Savin, C. J. Umrigar, X. Gonze, *Chem. Phys. Lett.* **1998**, *288*, 391.
[78] M. J. Frisch, G. W. Trucks, H. B. Schlegel, G. E. Scuseria, M. A. Robb, J. R. Cheeseman, J. A. Montgomery Jr, T. Vreven, K. N. Kudin, J. C. Burant, J. M. Millam, S. S. Iyengar, J. Tomasi, V. Barone, B. Mennucci, M. Cossi, G. Scalmani, N. Rega, G. Petersson, H. Nakatsuji, M. Hada, M. Ehara, K. Toyota, R. Fukuda, J. Hasegama, M. Ishida, T. Nakajima, Y. Honda, O. Kitao, H. Nakai, M. Klene, X. Li, J. E. Knox, P. Hratchian, J. B. Cross, C. Adamo, J. Jaramillo, R. Gomperts, R. E. Stratmann, O. Yazyev, A. J. Austin, R. Cammi, C. Pomelli, J. W. Ochterski, P. Y. Ayala, K. Morokuma, G. A. Voth, P. Salvador, J. J. Dannenberg, V. G. Zakrzewski, S. Dapprich, A. D. Daniels, M. C. Strain, O. Farkas, D. K. Malick, A. D. Rabuck, K. Raghavachari, J. B. Foresman, J. V. Ortiz, Q. Cui, A. G. Baboul, S. Clifford, J. Ciolowski, B. B. Stefanov, G. Liu, A. Liashenko, P. Piskorz, I. Komaromi, R. L. Martin, D. J. Fox, T. Keith, M. A. Al-Laham, C. Y. Peng, A. Nanayakkara, M. Challacombe, P. M. W. Gill, B. Johnson, W. Chen, M. W.Wong, C. Gonzales, J. A. Pople, *Gaussian 03*, *Revision B.02*, Gaussian, Inc., Pittsburgh, **2003**.
[79] a) T. Leininger, A. Nicklass, H. Stoll, M. Dolg, P. Schwerdtfeger, *J. Chem. Phys.* **1996**, *105*, 1052; b) H.-J. Werner, P. J. Knowles, *J. Chem. Phys.* **1985**, *82*, 5053; c) H.-J. Werner, P. J. Knowles, M. Schütz, R. Lindh, P. Celani, T. Korona, G. Rauhut, F. R. Manby, R. D. Amos, A. Bernhardsson, A. Berning, D. L. Cooper, M. J. O. Deegan, A. J. Dobbyn, F. Eckert, C. Hampel, G. Hetzer, A. W. Lloyd, S. J. McNicholas, W. Meyer, M. E. Mura, A. Nicklass, P. Palmieri, R. Pitzer, U. Schumann, H. Stoll, A. J. Stone, R. Tarroni, T. Thorsteinsson, *MOLPRO 2002.3: A Package of Ab Initio Programs.*
[80] a) T. H. Dunning Jr, *J. Chem. Phys.* **1989**, *90*, 1007; b) R. A. Kendall, T. H. Dunning Jr, R. J. Harrison, *J. Chem. Phys.* **1992**, *96*, 6796; c) D. E. Woon, T. H. Dunning Jr, *J. Chem. Phys.* **1993**, *98*, 1358.
[81] R. Zahradník, L. Šroubková, *Isr. J. Chem.* **2003**, *43*, 243.
[82] H. Nakatsuji, *Chem. Phys. Lett.* **1978**, *59*, 362.
[83] a) H.-J. Werner, P. J. Knowles, *J. Chem. Phys.* **1988**, *89*, 5803; b) P. J. Knowles, H.-J. Werner, *Chem. Phys. Lett.* **1988**, *145*, 514.
[84] a) M. Douglas, N. M. Kroll, *Ann. Phys. (N. Y)* **1974**, *82*, 89; b) B. A. Hess, *Phys. Rev. A* **1986**, *33*, 3742; c) G. Jansen, B. A. Hess, *Phys. Rev. A* **1989**, *39*, 6016; d) L. L. Foldy, S. A. Wonthuysen, *Phys. Rev.* **1950**, *78*, 29.
[85] N. Godbout, D. R. Salahub, J. Andzelm, E. Wimmer, *Can. J. Chem.* **1992**, *70*, 560.
[86] S. F. Boys, F. Bernardi, *Mol. Phys.* **1970**, *19*, 553.
[87] a) R. B. Ross, J. M. Powers, T. Atashroo, W. C. Ermler, L. A. LaJohn, P. A. Christiansen, *J. Chem. Phys.* **1990**, *93*, 6654; b) R. B. Ross, J. M. Powers, T. Atashroo, W. C. Ermler, L. A. LaJohn, P. A. Christiansen, *J. Chem. Phys.* **1994**, *101*, 1098.
[88] K. P. Huber, G. Herzberg, *Molecules Spectra and Molecular Structure IV: Constants of Diatomic Molecules*, Van Nostrand Reinold, New York, **1979**.
[89] A. A. Radzig, B. M. Smirnov, *Reference Data on Atoms, Molecules and Ions*, Springer, Berlin, **1985**.
[90] A. Costales, A. K. Kandalam, R. Franco, R. Pandey, *J. Phys. Chem. B* **2002**, *106*, 1940.
[91] R. A. Elber, C. Rotberg, C. Simmerling, R. Goldstein, H. Y. Li, G. Verkhivker, C. Keasar, J. Zhang, A. Ulitsky, *Comput. Phys. Commun.* **1995**, *91*, 159.
[92] J. J. P. Stewart, *J. Comput. Chem.* **1989**, *10*, 209.

[93] D. R. Lide, *Handbook of Chemistry and Physics*, 85th ed., CRC Press, New York, **2004**.
[94] J. M. Matxain, J. M. Ugalde, M. D. Towler, R. J. Needs, *J. Phys. Chem. A* **2003**, *107*, 10004.
[95] K. A. Peterson, *J. Chem. Phys.* **1995**, *102*, 262.
[96] T. E. Sorensen, W. B. England, *Int. J. Quantum Chem.* **2000**, *76*, 259.

Received: September 4, 2006
Published Online: February 28, 2007

